

# SRDA-Net: Super-Resolution Domain Adaptation Networks for Semantic Segmentation

Zhenjie Tang, Bin Pan, Enhai Liu, Xia Xu, Tianyang Shi, Zhenwei Shi

**Abstract**—Recently, Unsupervised Domain Adaptation (UDA) was proposed to address the domain shift problem in semantic segmentation task, but it may perform poor when source and target domains belong to different resolutions. In this work, we design a novel end-to-end semantic segmentation network, Super-Resolution Domain Adaptation Network (SRDA-Net), which could simultaneously complete super-resolution and domain adaptation. Such characteristics exactly meet the requirement of semantic segmentation for remote sensing images which usually involve various resolutions. Generally, SRDA-Net includes three deep neural networks: a super-Resolution and Segmentation (RS) model focuses on recovering high-resolution image and predicting segmentation map; a pixel-level domain classifier (PDC) tries to distinguish the images from which domains; and output-space domain classifier (ODC) discriminates pixel label distribution from which domains. PDC and ODC are considered as the discriminators, and RS is treated as the generator. By the adversarial learning, RS tries to align the source with target domains on pixel-level visual appearance and output-space. Experiments are conducted on the two remote sensing datasets with different resolutions. SRDA-Net performs favorably against the state-of-the-art methods in terms of the mIoU metric.

**Index Terms**—domain adaptation, super resolution, semantic segmentation

## I. INTRODUCTION

REMOTE sensing imagery semantic segmentation, which aims at assigning a semantic label for every pixel of an image, has enabled various high-level applications, such as urban planning, land-use survey and environment monitoring [1]–[3]. Recently, deep convolutional neural networks (CNNs) have presented amazing performance in the task of semantic segmentation [4]–[9]. However, to guarantee the superior representation ability of CNNs, a large amount of manually labeled data are required for training. The manually annotating process for each pixel is time-consuming and labor-intensive.

Unsupervised Domain Adaptation (UDA) is one of the powerful techniques to handle the problem of insufficient

The work was supported by Natural Science Foundation of Hebei Province (Grant No. F2019202062) and the Tianjin Science and Technology Project (Grant No. 18YFCZZC00060 and No. 18ZXZNGX00100).

Enhai Liu and Zhenjie Tang are with the School of Artificial Intelligence, Hebei University of Technology, Tianjin 300401, China, and also with the Hebei Province Key Laboratory of Big Data Calculation, Tianjin 300401, China (e-mail:liuanghai@scse.hebut.edu.cn; 201832102002@stu.hebut.edu.cn).

Bin Pan (Corresponding author) is with the School of Statistics and Data Science, Nankai University, Tianjin 300071, China (e-mail: panbin@nankai.edu.cn).

Xia Xu is with College of Computer Science, Nankai University, Tianjin 300350, China (e-mail: xuxia@nankai.edu.cn).

Tianyang Shi and Zhenwei Shi are with the Image Processing Center, School of Astronautics, Beihang University, Beijing 100191, China (e-mail: shitianyang@buaa.edu.cn; shizhenwei@buaa.edu.cn).

labeling. UDA is the field of research that aims at learning a well performance model of target domain from source supervision only. Most UDA works for semantic segmentation seek to align features in a deep network of source and target domains by either explicitly matching feature statistics [10] or implicitly making features domain invariant [11]–[14]. Recently, many works attempt to minimize domain shift at the pixel-level by turning source domain images into target-like images with adversarial training [12], [14]–[17]. There are also some researchers that propose to reduce the spatial structure domain discrepancies in the output space [18], [19].

However, UDA methods for natural scene images may not be directly transferred to remote sensing images, because of the problem of spatial resolution problem. Spatial resolution is one of the important characteristics of remote sensing images. Unlike natural scene images, the sensors used to acquire remote sensing images usually have significant differences, which results in different spatial resolutions. The definition of resolution in remote sensing image is not the same as that in natural scene. For example, there may be both large and small cars in a natural scene image, however, a car in a 4m-resolution remote sensing image can never be the same size as a car in a 1m-resolution image. On the other hand, if we only considered UDA for remote sensing images with the same resolution, the available data should be severely compressed. Therefore, we may conclude that UDA for remote sensing images should not only narrow the gaps between source and target domains, but also address the issue of different resolutions.

To the best of our knowledge, there are few UDA algorithms for remote sensing images that explicitly consider the resolution problem. Most UDA works dealt with the resolution problem by simply interpolation [20] or adjusting the parameters of kernel function [21]. When the domain gap of resolution between source and target domains is not serious, some researchers [22], [23] ignored the resolution problem. For instance, Yan et al. [22] proposed a triplet adversarial domain adaptation method to learn a domain-invariant classifier in output-space by a novel domain discriminator, which ignored the resolution problem between source and target domains. Instead of matching the distribution in output-space, Zhang et al. [20] developed to eliminate the domain shift by aligning the distributions of the source and target data in the feature space, which dealt with the resolution problem only by interpolation. Liu et al. [21] also minimized the distance of feature distributions between source and target domains through metric under different kernel functions, which reduce the effect of resolution problem by adjust the parameters of kernel function. However, the existing UDA methods for re-

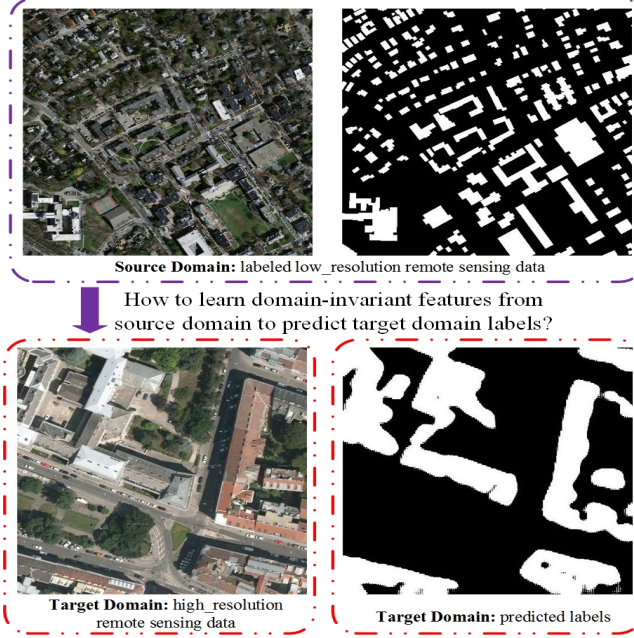


Fig. 1. A unsupervised domain adaptation approach for semantic segmentation in remote sensing images. Given a source domain (low-resolution remote sensing data) with labels, and a target domain (high-resolution remote sensing data) without labels, our goal is train a segmentation model to predict the labels of the target domain.

remote sensing images have not explicitly studied the resolution problem.

Explicitly considering the resolution problem, in this paper, we propose a novel end-to-end network that can simultaneously conduct Super-Resolution and Domain Adaptation (SRDA-Net), which improves the segmentation performance from low-resolution remote sensing data (source domain) to high-resolution remote sensing data (target domain). Fig. 1 briefly depicts the problem setting: source domain (low-resolution remote sensing images) with labels and target domain (high-resolution remote sensing images) without labels. SRDA-Net is motivated by two recent research: 1) adversarial training based UDA methods for semantic segmentation 2) super-resolution and semantic segmentation can promote each other. Recently, most of the UDA methods resort to adversarial training to reduce the domain discrepancies. For instance, Zhang et al. [12] apply the adversarial loss to the lower layers of segmentation network because the lower layers mainly capture the appearance information of the images. Tsai et al. [18] employ the adversarial feature learning in the output space over the base segmentation model. Hung Vu et al. [19] also reduce the discrepancies of feature distributions in output space through Adversarial Entropy Minimization. Moreover, recent research show that super-resolution and semantic segmentation can boost each other. Some researchers recently show that super-resolution results can be improved by semantic priors, such as semantic segmentation probability maps [24] or segmentation labels [25]. In the field of remote sensing, high-resolution images which contain many details are important for image segmentation [26]. For instance, Lei et al. [26] propose to combine image super-resolution in

segmentation network to obtain improvements on both super-resolution and segmentation tasks.

To be specific, the SRDA-Net consists of three deep neural networks, a multi-task model for super-Resolution and semantic Segmentation (RS), a Pixel-level Domain Classifier (PDC) and Output-space Domain Classifier (ODC). RS integrates a super-resolution network and a segmentation network into one architecture. The former focuses on recovering the high-resolution images with the style of target domain, and the latter aims to get the segmentation result with aligned in output-space [18]. PDC is fed with high-resolution images of super-resolution network, and outputs their domain (source or target domain) for each pixel. ODC is fed with the predicted label distributions of segmentation network, then outputs the domain class for each pixel label distribution. Similar to generative adversarial networks(GANs) [27], RS model can be regarded as a generator, and PDC/ODC models are treated as two discriminators. Through adversarial training, RS model can learn domain-invariant features at the pixel and output-space levels.

In summary, our major contributions of SRDA-Net can be summarized as follows:

- A new UDA method named SRDA-Net is proposed for semantic segmentation to adapt from low-resolution remote sensing images to high-resolution remote sensing images.
- Inspired by the mutual promotion of super-resolution and semantic segmentation, we construct a multi-task model composed of super-resolution and segmentation, which not only eliminates the resolution difference between source and target domains, but also obtains improvements on both super-resolution and segmentation tasks.
- We design two domain classifiers at the pixel-level and output space to align the source and target domains. By adversarial training, the domain gap can be effectively reduced.

## II. RELATED WORK

In this section, we briefly review the important works: semantic segmentation, single image super resolution, unsupervised domain adaptation.

### A. Semantic Segmentation

Semantic segmentation is the task that assigns each pixel a semantic label for an image which plays a vital role in lots of tasks including autonomous driving, urban planning, etc. In 2014, fully convolutional network (FCN) [4] presents amazing performance in the field of some pixel-wise tasks (such as semantic segmentation). After that, models based on Fully Convolutional Networks (FCNs) have demonstrated significant improvement on several segmentation benchmarks [28], [29]. There are several model variants proposed to exploit the contextual information for segmentation by adopting multi-scale inputs [7], [30] or employing probabilistic graphical models [31]. For instance, Chen et al. [7] propose a dilated convolution operation to aggregate multi-scale contextual information. Zhao et al. [6] introduce a pyramid pooling module

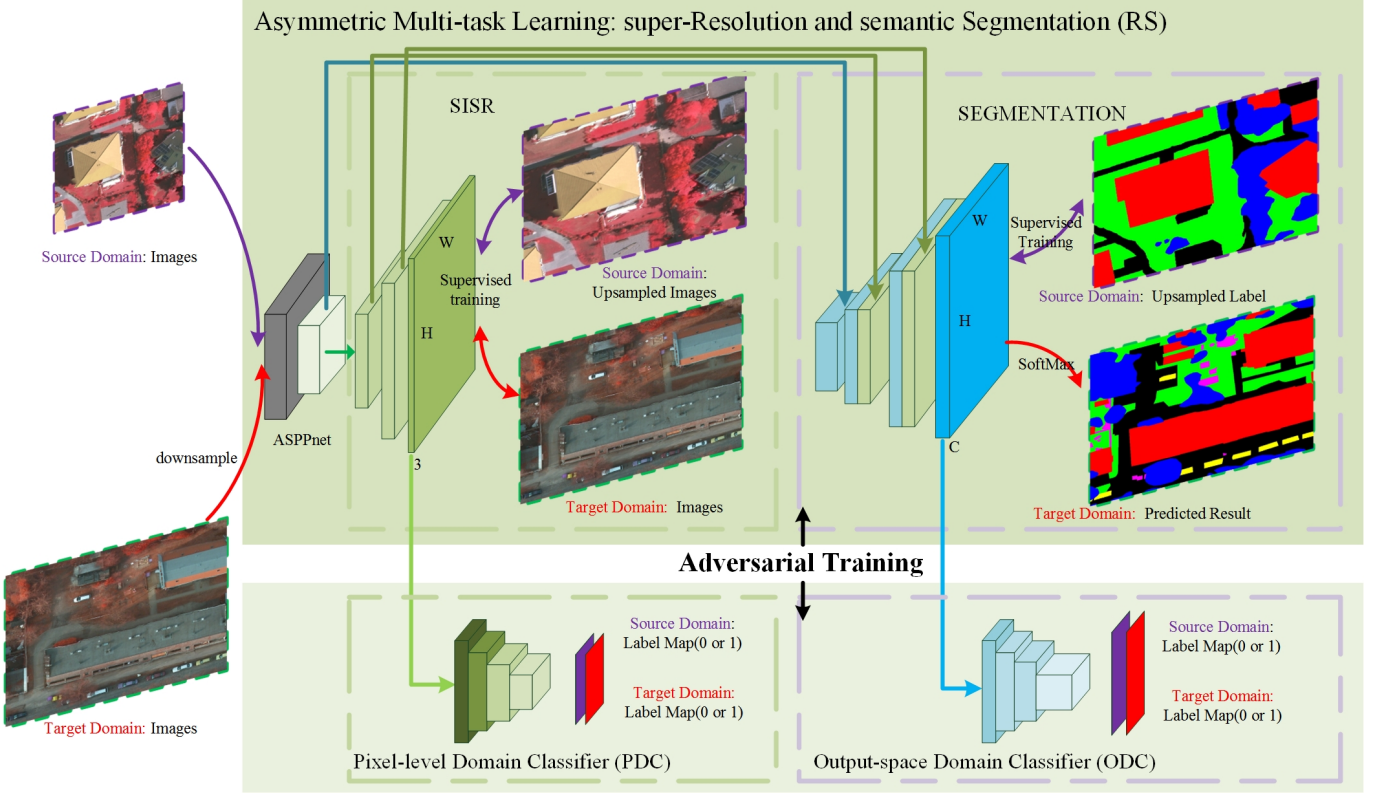


Fig. 2. The overview of our Super-Resolution Domain Adaptation Network (SRDA-Net). On the top, the asymmetric multi-task model is depicted, which consists of a super-Resolution model and a Segmentation model (RS). During the training phase, the source domain image and downsampled target domain image are fed to the RS model. The purple and red curve arrows respectively represent the input/output of source and target domain. Further, the two-way arrow indicates the data flow involved in the training process. From this figure, source images take part in the super-resolution and segmentation training in the supervised manner, while target images only participate the super-resolution training in the supervised manner. On the bottom, the Pixel-level Domain Classifier (PDC) and Output-space Domain Classifier (ODC) are demonstrated. The Super-Resolution images and the predicted label distributions from RS are respectively flowed to PDC and ODC. By adversarial training RS and the two classifiers, the final RS will be obtained. During the testing stage, the downsampled test images are fed to the RS for predicting the segmentation map.

in FCN to exploit the contextual information. Recently, Lei et al. [26] also propose to combine image super-resolution in segmentation network to obtain improvements on both super-resolution and segmentation tasks.

### B. Single Image Super Resolution

Single Image Super Resolution (SISR) [32] aims to recover high-resolution images from the corresponding low-resolution ones, which has been widely used in many applications such as security and surveillance imaging, medical imaging and remote sensing image reconstruction. The conventional non-CNN methods mainly focused on the domain and feature priors. For example, interpolation methods such as bicubic and Lanczos generate the HR pixels by the weighted average of neighboring LR pixels. Recently, CNN-based methods [33]–[35] consider SISR as a mapping between the LR and HR spaces in an end-to-end manner, showing great breakthrough. Also, some researchers use perceptual loss [36], [37] and adversarial training to improve perceptual quality of SISR.

### C. Unsupervised Domain Adaptation

Since we are only concerned with visual semantic segmentation in this work, we limit our review of UDA to approaches

that aim at this task as well. Many UDA approaches [11]–[14] for segmentation employ adversarial training to minimize cross-domain discrepancy in the feature space. Another works [18], [19] proposed alignment the predicted label distributions in the output space. Tsai et al. [18] do the alignment on the prediction of the segmentation network and Vu et al. [19] propose to do it on entropy minimization of the prediction probability. In contrast, pixel-level domain adaptation [16], [38] is the use of generative networks to turn source domain images into target-like images. Li et al. [16] present a bidirectional learning system for semantic segmentation, which is a closed loop to learn the segmentation adaptation model and the image translation model alternatively, causing the domain gap to be gradually reduced at the pixel-level. Recently, a curriculum learning strategy is proposed in [39]–[41] by leveraging information from global label distributions and local super-pixel distributions of target domain. Besides, some works use some privileged information to guide the segmentation learning (i.e., PI [42] and dense depth [17]).

## III. APPROACH

This section describes the detailed methodology of the proposed unsupervised domain adaptation for semantic segmentation. In order to reduce the domain gap (including the

resolution difference), we integrate the super-resolution to segmentation model for eliminating the impact of different resolutions. Moreover, by adversarial optimizing RS and two domain classifiers (PDC and ODC), the domain gap in pixel-level and output-space can be gradually reduced. Fig. 2 shows the entire framework.

Before illustrating the method in detail, it is necessary to define our faced the cross-domain problem with mathematical notations. A source domain  $\mathcal{S}$  from a low-resolution remote sensing dataset provides low-resolution images  $I_{\mathcal{S}}$ , pixel-level annotations  $A_{\mathcal{S}}$ ; a target domain  $\mathcal{T}$  from high-resolution remote sensing dataset only provides high-resolution images  $I_{\mathcal{T}}$ . Note that  $\mathcal{S}$  and  $\mathcal{T}$  share the same label space  $\mathbb{R}^C$ , where the  $C$  denotes the number of categories. In a word, given  $I_{\mathcal{S}}$ ,  $A_{\mathcal{S}}$ ,  $I_{\mathcal{T}}$ , our goal is to learn a segmentation model to predict pixel-wise category of  $\mathcal{T}$ .

According to the definition above, the purpose of this paper is that how to reduce the domain gap (including resolution difference) between  $\mathcal{S}$  and  $\mathcal{T}$ . Below, we first describe the asymmetric multi-task (super-resolution and segmentation) model. Then, the Adversarial Domain Adaptation (Pixel-Level and output-space) is presented in details.

#### A. Multi-task Model: Super-Resolution and Segmentation

Over the past few years, methods based on convolutional neural networks (CNNs) have achieved significant progress in semantic segmentation. However, CNN-based methods may not generalize well to unseen images, especially when there is a domain gap between the training (source domain) and test (target domain) images. For remote sensing images, the resolution difference is a important domain gap, which seriously affects the generalization ability of the segmentation model. Thus, it is important to eliminate resolution difference for cross-domain semantic segmentation in remote sensing.

Recently, some researchers [24], [26] show that super-resolution and semantic segmentation can boost each other. Therefore, super-resolution and segmentation both are challenging tasks, but they may have certain relationship. Super-resolution will provide images with more details that may help to improve the segmentation accuracy, while label maps in segmentation dataset or semantic segmentation probability maps may contribute to recover textures faithful to semantic classes during super-resolution process.

Based on the above discussions, we propose an asymmetric multi-task learning model to eliminate the gap of different resolution between source and target domains, which consists of super-Resolution and Segmentation models (RS). In order to make super-resolution and segmentation boost each other, we propose two strategies: (1) we introduce a pyramid feature fusion structure between the two tasks; (2) for the generated high-resolution images of source domain, we impose the cross-entropy segmentation loss to train the segmentation network. During the training phase, the source domain image and downsampled target domain image are fed to the RS network: the source domain image is involved in the entire training process; the target image only participates in the Super-Resolution training process (shown in Fig. 2). At the testing

stage, the downsampled test images are fed to RS network to obtain the pixel-wise scope maps.

To be specific, we employ Residual ASPP Module [43] as the shared feature extractor. For the super-resolution model, due to GPU memory limitation, we only use a few deconvolutions to recover the high-resolution images without using pixelshuffle [44]. In order to transfer the low-level features from super-resolution stream to segmentation stream, we introduce the pyramid feature fusion structure [45] between the two streams. Moreover, the super-resolution results of source domain are also fed to the segmentation stream. Meanwhile, the segmentation stream also ensures to recover textures faithful to semantic classes during super-resolution stream.

The proposed RS model is trained through following loss:

$$\mathcal{L}_{RS} = \alpha \mathcal{L}_{seg} + \beta (\mathcal{L}_{idT} + \mathcal{L}_{ids}) \quad (1)$$

$$\mathcal{L}_{seg} = \mathcal{L}_{cel} (\mathbf{S}(I_{\mathcal{S}}), \uparrow A_{\mathcal{S}}) + \mathcal{L}_{cel} (\mathbf{S}(\downarrow \mathbf{R}(I_{\mathcal{S}})), \uparrow A_{\mathcal{S}}) \quad (2)$$

$$\mathcal{L}_{idT} = \mathcal{L}_{mse} (\mathbf{R}(\downarrow I_{\mathcal{T}}), I_{\mathcal{T}}) \quad (3)$$

$$\mathcal{L}_{ids} = \mathcal{L}_{per} (\mathbf{R}(I_{\mathcal{S}}), \uparrow I_{\mathcal{S}}) + 0.5 \times \mathcal{L}_{fp} \quad (4)$$

$$\mathcal{L}_{fp} = \mathcal{L}_{L1} (\mathbf{E}(\downarrow \mathbf{R}(I_{\mathcal{S}})), \mathbf{E}(I_{\mathcal{S}})) \quad (5)$$

where  $\mathcal{L}_{cel}$  is the 2D Cross Entropy Loss, the standard supervised pixel-wise classification objective function;  $\mathcal{L}_{mse}$  is the pixel-wise MSE loss, the most widely used optimization target for image SISR;  $\mathcal{L}_{per}$  is the perceptual loss [36];  $\mathcal{L}_{L1}$  is the L1 norm loss. The  $\uparrow$  and  $\downarrow$  denote upsampling and downsampling operations, respectively.  $\mathbf{S}$ ,  $\mathbf{R}$ , and  $\mathbf{E}$  denote Segmentation model ( $\mathbf{S}$ ), super-Resolution model ( $\mathbf{R}$ ) and the shared feature Extractor ( $\mathbf{E}$ ), respectively. Note that, in order to easily superimpose the style of target domain, we use the  $\mathcal{L}_{per}$  and  $\mathcal{L}_{fp}$  (fixpoint loss [46]) to train the super-resolution model of source domain images.  $\alpha$ ,  $\beta$  denote the weighting factors for semantic segmentation and super-resolution.

#### B. Adversarial Domain Adaptation

Although the proposed asymmetric multi-task model eliminates the resolution difference between source and target domains, other domain gaps (such as texture, color and so on) are still not alleviated. Due to the influence of sensors, geographic locations, imaging conditions, and other factors, these differences are inherent in remote sensing imagery. For traditional supervised deep learning, the model only learns to the discriminative features based on the given annotated remote sensing data. Therefore, there is a problem that how to learn the domain-invariant features for remote sensing imagery.

Adversarial learning provides a good framework to deal with the problem, which consists of a generator network and a discriminator network. The main idea is to train the discriminator for predicting the domain of the data (source or target domain) while the segmentation network tries to fool it (along with the supervised segmentation task on the source). Through alternately training the two networks, the feature domain gap can be gradually reduced.

In this paper, we design the pixel-level and output-space Domain Classifiers (PDC and ODC) as discriminators, and the RS treated as the generator. By the adversarial training, RS will learn the domain-invariant features that fool the PDC and ODC.

### C. Pixel-Level Adaptation

Since the proposed multi-task mode (RS) only eliminates the resolution difference between source and target domains and does not reduce the gap in appearance, a pixel-level domain classifier (PDC) is built to distinguish the domain category for each pixel. It receives the high-resolution images of source or target domain. To be specific, we apply the PatchGAN [47] as PDC. The bottom-left sub figure in Fig. 2 shows the network architecture of PDC.

The PDC loss is computed as follows:

$$I_S^R = \mathbf{R}(I_S) \in \mathbb{R}^{H \times W \times 3} \quad (6)$$

$$I_{fake} = \mathbf{D}_{pdc}(I_S^R) \in \mathbb{R}^{H \times W \times 1} \quad (7)$$

$$I_{true} = \mathbf{D}_{pdc}(I_T) \in \mathbb{R}^{H \times W \times 1} \quad (8)$$

$$\begin{aligned} \mathcal{L}_{PDC} = & \mathbb{E}_{I_{fake} \sim p_{data}(I_{fake})} [(I_{fake} - 1)^2] \\ & + \mathbb{E}_{I_{true} \sim p_{data}(I_{true})} [(I_{true})^2] \end{aligned} \quad (9)$$

where  $\mathbf{D}_{pdc}$  is the pixel-level domain classifier model,  $H$  and  $W$  denote the height and width of the high-resolution target domain image.

At the same time, the inverse of PDC loss is defined as:

$$\begin{aligned} \mathcal{L}_{PDC_{inv}} = & \mathbb{E}_{I_{true} \sim p_{data}(I_{true})} [(I_{true} - 1)^2] \\ & + \mathbb{E}_{I_{fake} \sim p_{data}(I_{fake})} [(I_{fake})^2] \end{aligned} \quad (10)$$

Finally, the adversarial objective functions are written as follows:

$$\min_{\theta_{RS}} \mathcal{L}_{RS} + \mathcal{L}_{PDC} \quad (11)$$

$$\min_{\theta_{PDC}} \mathcal{L}_{PDC_{inv}} \quad (12)$$

where  $\theta_{RS}$  and  $\theta_{PDC}$  denote the network parameters of RS and PDC, respectively. During the training phase, the parameters of the two models are updated in turns using Eq.(11) and Eq.(12).

### D. Output-Space Adaptation

Different from image classification task that based on global features, the generated high-dimensional features for semantic segmentation encode complex representations. Therefore, adaptation only in the pixel space may not enough for semantic segmentation. On the other hand, although segmentation outputs are in the low-dimensional space, they contain rich information, e.g., scene layout and context. Moreover, in remote sensing scenes, no matter images are from the source or target domain, their segmentations should share strong similarities, spatially and locally. For example, the rectangular road region may cover the part of cars, pedestrians; and the green plants

often grow around the buildings. Thus, we adapt the low-dimensional softmax outputs of segmentation predictions via an adversarial learning scheme.

To be specific, we design a output-space Domain Classifier (ODC) to distinguish domain source (source domain or target domain) for each pixel label distribution, which receives the segmentation softmax output:  $P = \mathbf{S}(I) \in \mathbb{R}^{H \times W \times C}$ , where  $C$  is the number of categories. We forward  $P$  to output-space Domain Classifier model  $\mathbf{D}_{odc}$  using a cross-entropy loss  $\mathcal{L}_{ODC}$  for the two classes (i.e., source and target). The ODC loss can be written as:

$$P_S = \mathbf{S}(I_S) \in \mathbb{R}^{H \times W \times C} \quad (13)$$

$$P_T = \mathbf{S}(\downarrow I_T) \in \mathbb{R}^{H \times W \times C} \quad (14)$$

$$P_{true} = \mathbf{D}_{odc}(P_S) \in \mathbb{R}^{H \times W \times 1} \quad (15)$$

$$P_{fake} = \mathbf{D}_{odc}(P_T) \in \mathbb{R}^{H \times W \times 1} \quad (16)$$

$$\mathcal{L}_{ODC} = - \sum_{h,w} (1-z) \log(P_{fake}) + z \log(P_{true}) \quad (17)$$

The inverse of ODC loss is defined as:

$$\mathcal{L}_{ODC_{inv}} = - \sum_{h,w} (1-z) \log(P_{true}) + z \log(P_{fake}) \quad (18)$$

In the end, the adversarial objective functions are computed as follows:

$$\min_{\theta_{RS}} \mathcal{L}_{RS} + \mathcal{L}_{ODC} \quad (19)$$

$$\min_{\theta_{ODC}} \mathcal{L}_{ODC_{inv}} \quad (20)$$

where  $\theta_{RS}$  and  $\theta_{ODC}$  denote the parameters of RS and ODC networks, respectively. During the training stage, the parameters of two networks are updated in turns by minimizing Eq.(19) and Eq.(20).

### E. Final objective function

In order to make the network have a good initialization parameters, we first use the following loss function for pre-training:

$$\min_{\theta_R} \beta (\mathcal{L}_{idT} + \mathcal{L}_{idS}) + \mathcal{L}_{PDC} \quad (21)$$

$$\min_{\theta_{PDC}} \mathcal{L}_{PDC_{inv}} \quad (22)$$

where  $\beta$  denotes a weighting factor for super-resolution,  $\theta_R$  is the parameters of super-Resolution ( $\mathbf{R}$ ) network. During training stage, the  $\mathbf{R}$  and PDC networks are optimized in turns using Eq.(21) and Eq.(22).

For the full models (including RS, PDC and ODC) training, our full objective can be formulated as:

$$\min_{\theta_{RS}} \mathcal{L}_{RS} + \mathcal{L}_{PDC} + \mathcal{L}_{ODC} \quad (23)$$

$$\min_{\theta_d} \mathcal{L}_{PDC_{inv}} + \mathcal{L}_{ODC_{inv}} \quad (24)$$

where  $\theta_d$  denotes the network parameters of PDC and ODC. During training phase, the parameters of RS, PDC and ODC are optimized in turns by minimizing Eq.(23) and Eq.(24). Algorithm 1 illustrates training procedure of our proposed SRDA-Net.

---

**Algorithm 1** the proposed SRDA-Net.

---

**Input:**

Data: Source Domain low-resolution image  $I_S$ , Target Domain high-resolution image  $I_T$ , Source Domain low-resolution label  $A_S$   
 Parameter:  $\beta = 10, \alpha$

**Output:**

High-resolution source domain image with style of target domain:  $I_S^R$

Predict label of target domain:  $A_T$

**Repeat**

- 2: % Super-Resolution images by the **R** model  
 $I_S^R, I_T^R = \mathbf{R}(I_S, \downarrow I_T) \in \mathbb{R}^{H \times W \times 3}$
- 3: % Segmentation softmax outputs from the **S** model  
 $P_S, P_T = \mathbf{S}(I_S, \downarrow I_T) \in \mathbb{R}^{H \times W \times C}$
- 4: % Predict label of target domain image  
 $A_T = \max(P_T) \in \mathbb{R}^{H \times W \times 1}$
- 5: % Distinguish the pixels of super-resolution images  
 $I_{fake}, I_{true} = \mathbf{D}_{pdc}(I_S^R, I_T) \in \mathbb{R}^{H \times W \times 1}$
- 6: % Distinguish the pixel distributions of softmax outputs  
 $P_{true}, P_{fake} = \mathbf{D}_{odc}(P_S, P_T) \in \mathbb{R}^{H \times W \times 1}$
- 7: % Adversarial training  
**R** and **S** can be optimized according to equation (23).  
 $\mathbf{D}_{pdc}$  and  $\mathbf{D}_{odc}$  are updated by minimizing the inverse loss (24).
- 8: **Until** convergence
- 9: Obtain an adaptive multi-task model: **RS**

---

## IV. EXPERIMENTS

In this section, we first introduce the two datasets we constructed: Mass-Inria Dataset and Vaih-Pots Dataset. Then, the experimental setup and implementation details are presented. Next, extensive experimental results are shown to demonstrate the effectiveness of our method on the two datasets. Finally, the super-resolution results with style transfer of source domain images from CycleGAN and SRDA-Net are presented, which confirm that the semantic prior of segmentation improves the perform of super-resolution.

### A. Datasets

With the development of deep learning in remote sensing, there have been many large remote sensing datasets with different resolutions. Based on this, we constructed two datasets: a single-category Mass-Inria Dataset, and a multi-category Vaih-Pots Dataset.

1) *Mass-Inria*: We use the following two UDA datasets for single-category semantic segmentation.

- **Massachusetts Buildings Dataset** [48] consists of 151 aerial images of the Boston area, with each of the images being  $1500 \times 1500$  pixels for an area of 2.25 square kilometers (1m<sup>2</sup>/pixel). The ground truth provides two semantic classes (building and nonbuilding). The dataset is divided into a training set of 137 images, a test set of 10 images and a validation set of 4 images. We consider the training set of this dataset as the source domain.

- **Inria Aerial Image Labeling Dataset** [49] is comprised of 360 ortho-rectified aerial RGB images at 0.3m spatial resolution. The satellite scenes have tiles of size  $5000 \times 5000$  px, thus covering a surface of  $1500 \times 1500$ m per tile. Ground-truth provides two semantic classes (building and nonbuilding). The ground truth is only provided for the training set which covers five cities. We split the dataset (image 1 to 5 of each location for validation, 6 to 36 for training). We consider the training set of this dataset as target domain. We finally validate the results of the algorithm on the validation set of this dataset.

2) *Vaih-Pots*: We use the following two UDA datasets for multi-category semantic segmentation.

- **ISPRS Vaihingen 2D Semantic Labeling Challenge** is a widely used large-scale dataset for semantic labeling in aerial images. It contains 33 images of about  $2500 \times 2000$  pixels at a GSD of 9 cm, taken over the city of Vaihingen (Germany). All images have corresponding ground truth images. There are 6 labeled categories: impervious surface, building, low vegetation, tree, car, Clutter/background. We consider this dataset as source domain.

- **ISPRS Potsdam 2D Semantic Labeling Challenge dataset** is comprised of 38 ortho-rectified aerial IRRGB images ( $6000 \times 6000$  px) at 5cm spatial resolution, taken over the city of Potsdam (Germany). A comprehensive pixel-level ground truth is provided for 24 tiles with annotations of six classes alike Vaihingen dataset.

**Note that** the resolution gap of Mass-Inria (around 3.333 times) is greater than Vaih-Pots (around 2.0 times).

### B. Evaluation and Experimental Setup

1) *Evaluation*: In the semantic segmentation field, the intersection-over-union (IoU) is adopted as the main evaluation metric. Its defined by:

$$\text{IoU}(P_m, P_{gt}) = \left| \frac{P_m \cap P_{gt}}{P_m \cup P_{gt}} \right| \quad (25)$$

where  $P_m$  is the prediction and  $P_{gt}$  is the ground truth. Mean IoU (mIoU) is used to evaluate model performance on all classes.

2) *Experimental Setup: Network architectures*: In RS, we choose the Residual ASPP Module [43] to capture contextual information, as the shared feature Extractor. Moreover, we increase the number of channels to improve the ability to extract features. For the super-resolution stream, due to GPU memory limitation, we only use a few deconvolutions to recover the high-resolution images. In order to obtain a better performance for segmentation, we introduce a pyramid feature fusion structure [45] between the two tasks. As for two discriminators, we apply the PatchGAN [47] classifier as the PDC Network, and for ODC network we choose is similar to [18] which consists of 5 convolution layers with kernel 4 4 and stride of 2, where the channel number is 64, 128, 256, 512, 1, respectively.

**Training Details**: During training, adam optimization is applied with a momentum of 0.9. For the Mass to Inria, we

TABLE I  
DOMAIN ADAPTATION FROM MASS TO INRIA VAL DATASET: THE COMPARISON RESULTS OF THE STATE OF ART METHODS AND OURS

Methods %	BaseNet	Source domain	Target domain	IoU
NoAdapt [18]	Resnet-101 [50]	Mass	Inria	32.9
AdaptSegNet [18]	Resnet-101 [50]	Mass	↓ Inria	35.0
AdaptSegNet [18]	Resnet-101 [50]	↑ Mass	Inria	48.5
NoAdapt [12]	Resnet-101 [50]	Mass	Inria	32.9
CycleGan-FCAN [12]	Resnet-101 [50]	Mass	↓ Inria	41.8
CycleGan-FCAN [12]	Resnet-101 [50]	↑ Mass	Inria	49.7
RS (NoAdapt)	ResidualASPP [43]	Mass	Inria	36.7
RS + PDC	ResidualASPP [43]	Mass	Inria	46.0
RS + ODC	ResidualASPP [43]	Mass	Inria	39.4
Full (SRDA-Net)	ResidualASPP [43]	Mass	Inria	<b>52.8</b>

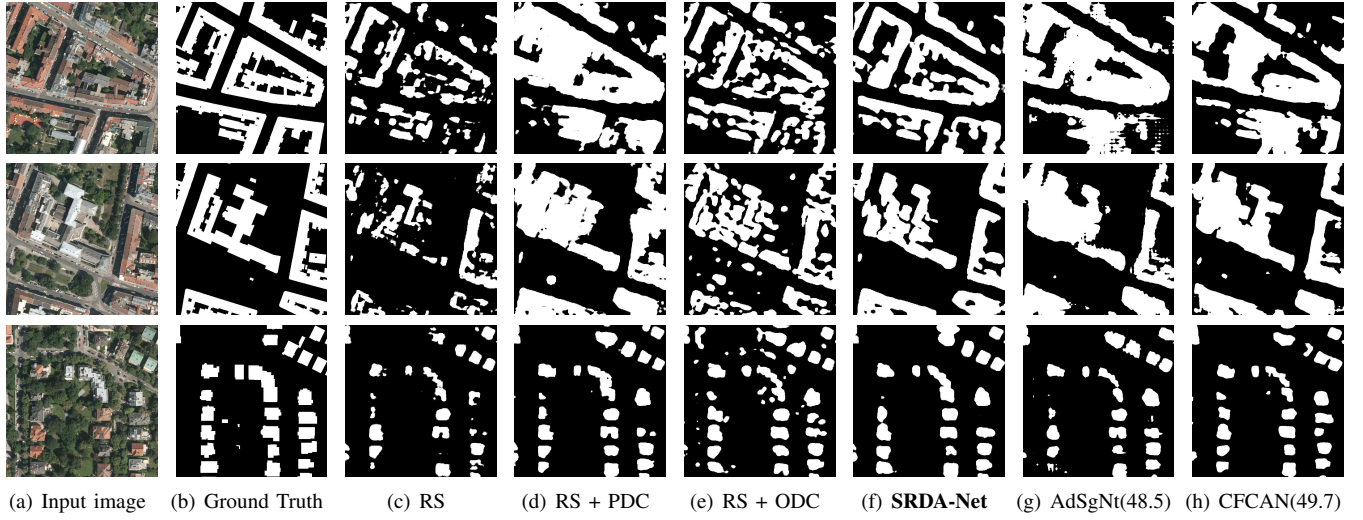


Fig. 3. Examples results of the Inria val dataset (Source domain: Massachusetts Buildings)

fix  $\alpha$  to 2.5,  $\beta$  to 10. Due to different resolution, the Mass images and labels are cropped  $114 \times 114$  pixels and then the labels are interpolated to  $380 \times 380$  pixels. The Inria images are cropped  $380 \times 380$  pixels and resized to  $114 \times 114$  pixels. During testing, images of Inria are cropped to  $625 \times 625$  patches without overlap and resized to  $188 \times 188$ . In the Vaih to Pots experiments,  $\alpha = 5$ ,  $\beta = 10$ ; the low-resolution image is cropped to  $160 \times 160$  pixels and the high-resolution is cropped to  $320 \times 320$  pixels during training stage. During testing, images of Pots are cropped to  $500 \times 500$  pixels without overlap and resized to  $250 \times 250$  pixels. In the actual training process, in order to make the network have a good initialization parameters, we first train (8) with learning rate  $2 \times 10^{-4}$ . Then the framework is trained with the learning rate  $1.5 \times 10^{-4}$ .

### Our stepwise experiments.

- **RS:** RS is directly trained without domain adaptation from the source domain to the target domain.

- **RS + PDC:** Based on RS model, PDC is added to the training process by the adversarial learning.
- **RS + ODC:** Based on RS model, ODC is added to the training process by the adversarial learning.
- **SRDA-Net (RS + PDC + ODC):** the proposed SRDA-Net model.

### Other comparison experiments.

- **AdaptSegNet [18]:** This work employs the adversarial feature learning in output-space of the base segmentation model. Instead of having only one discriminator over the feature layer, Tsai et al. propose to install another discriminator on one of the intermediate layers as well. Essentially, features of different scales are forced to align.
- **CycleGan-FCAN:** FCAN [12] is a two-stage method. AAN first adapts source-domain images to appear as if drawn from the style in the target domain, then RAN attempts to learn domain-invariant representations. To better adapt the source images to appear as if drawn from the target domain, we replace AAN in FCAN with

TABLE II  
DOMAIN ADAPTATION FROM VAIH TO POTS VAL DATASET: THE COMPARISON RESULTS OF THE STATE OF ART METHODS AND OURS

Methods %	BaseNet	Source	Target	Impervious	Building	vegetation	Tree	Car	Clutter	mIoU
NoAdapt [18]	Resnet-101 [50]	Vaih	Pots	51.8	45.5	46.2	11.8	35.3	18.5	34.9
AdaptSegNet [18]	Resnet-101 [50]	Vaih	↓ Pots	59.4	54.2	47.0	26.3	52.2	<b>32.2</b>	45.2
AdaptSegNet [18]	Resnet-101 [50]	↑ Vaih	Pots	55.1	55.6	43.0	31.5	60.6	1.6	41.2
NoAdapt [12]	Resnet-101 [50]	Vaih	Pots	51.8	45.5	46.2	11.8	35.3	18.5	34.9
CycleGan-FCAN [12]	Resnet-101 [50]	Vaih	↓ Pots	50.1	42.5	33.1	31.6	44.1	22.6	37.3
CycleGan-FCAN [12]	Resnet-101 [50]	↑ Vaih	Pots	47.9	51.2	43.0	41.7	61.1	23.8	44.8
RS (NoAdapt)	ResidualASPP [43]	Vaih	Pots	26.5	32.0	35.2	17.3	32.0	17.5	26.7
RS + PDC	ResidualASPP [43]	Vaih	Pots	58.3	51.1	51.8	27.9	62.5	20.5	45.4
RS + ODC	ResidualASPP [43]	Vaih	Pots	51.2	21.7	17.9	12.3	54.2	13.0	28.4
Full (SRDA-Net)	ResidualASPP [43]	Vaih	Pots	<b>60.2</b>	<b>61.0</b>	<b>51.8</b>	<b>36.8</b>	<b>63.4</b>	18.3	<b>48.6</b>

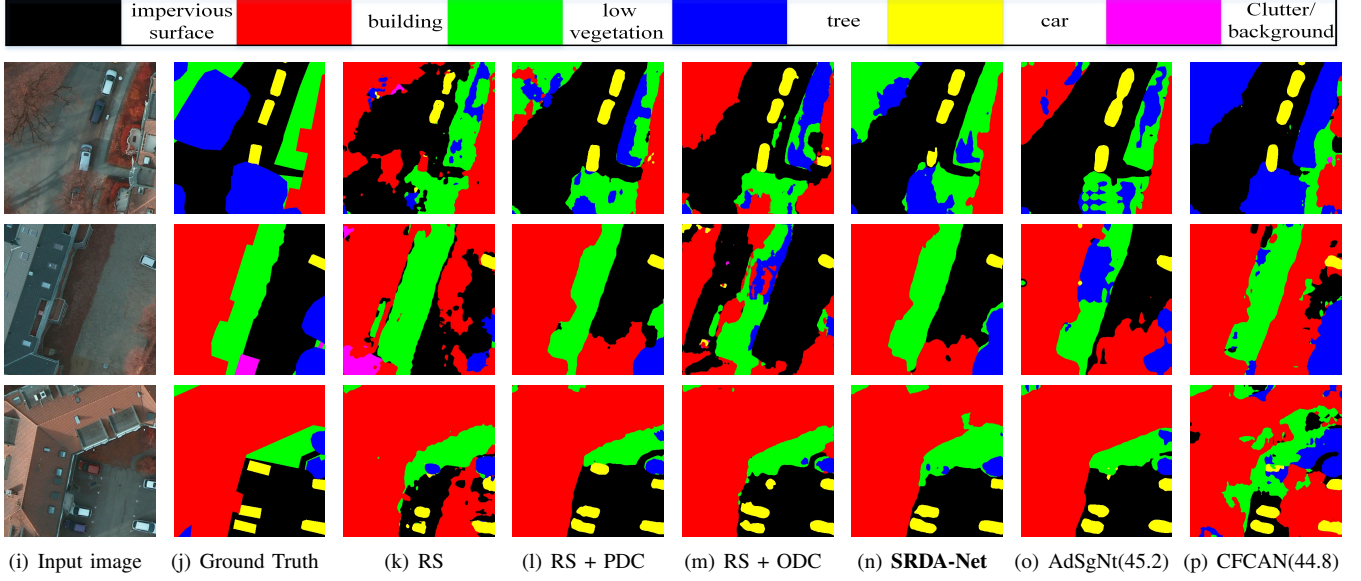


Fig. 4. Examples results of the Pots val dataset (Source domain: ISPRS Vaihingen 2D Semantic dataset)

cyclegan [51].

In the experiments, their non-adaptability and final result are listed for comparison with our stepwise experiments.

### C. Mass → Inria

Table I summarizes the qualitative results of some methods for the shift from Mass to Inria, including AdaptSegNet [18], CycleGan-FCAN [12] and our stepwise experiments: RS, RS + PDC, RS + ODC, SRDA-Net. The bold values denote the best scores in the column.

From the results, we can see that our proposed method (SRDA-Net) achieved the best result: IoU of 52.8%. Based on the same training strategy, result (52.8%) of SRDA-Net outperforms that of AdaptSegNet (best result of 48.5%) and

CycleGan-FCAN (best result of 49.7%). As for the results of the three methods with no adaptation, RS improves the IoU (from 32.9% to 36.7%, increasing by 3.8%) significantly, which shows the effectiveness of combining image super-resolution in segmentation network.

Further, the adaptation results of the three methods outperform their corresponding results of NoAdapt. Moreover, in order to explore the effect of resolution difference on the domain adaptation results, we construct experiments on two training data settings (source domain: Mass, target domain: Downsampled Inria; source domain: Upsampled Mass, target domain: Inria) for each comparison method. From the results, we find that the setting (source domain: Upsampled Mass, target domain: Inria) achieves more better result, which confirms that when the resolution difference between the source



Fig. 5. Examples results of super-resolution with style transfer from CycleGAN and SRDA-Net (upsampled source domain images  $\rightarrow$  target domain images)

and target domains is larger, the gain obtained by eliminating the resolution difference is greater than the error introduced by interpolation. In comparison, our method does not need to consider this, and obtained better results.

In order to explore the semantic segmentation performance further, Fig. 3 shows the visualization results of our step-by-step and the AdaptSegNet/CycleGan-FCAN methods. The images in the first column are selected from the Inria val dataset. The second column shows the ground truth, and the remaining columns illustrate the predicted results of RS, RS + PDC, RS + ODC, SRDA-Net, AdaptSegNet (48.5), CycleGan-FCAN (49.7). On the whole, after adding the PDC or ODC, some segmentation mistakes are removed effectively. According to the results of RS + PDC and RS + ODC, PDC plays a more important role in learning domain-invariant features than ODC (improvement of 9.3% versus 2.7%). When the domain gap is reduced by integrating PDC and ODC to RS, a better segmentation result can be obtained. Moreover, we can observe that the visualization segmentation results of SRDA-Net outperform results of best AdaptSegNet/CycleGan-FCAN.

#### D. Vaih $\rightarrow$ Pots

The results of AdaptSegNet [18], CycleGan-FCAN [12] and our stepwise experiments are listed in Table II, which are adapted from Vaih to Pots. The bold fonts represent the best scores of the corresponding columns. We observe that the proposed method obtains the best performance (48.6%). Compared with the previous best method AdaptSegNet (45.2%), the result of SRDA-Net contributes 3.4% relative mIoU improvement. For the three no adaptation methods, mIoU of our method is slightly lower. This is because that our parameters are less than half of resnet101, which limits the learning power of network. According to the mIoUs of DS+PDC and RS + ODC, PDCs contribution(18.7%) is greater than ODCs (1.7%).

From the results of comparison experiments, we find that when the gap of resolution between source and target domains is relatively small, it is difficult to determine whether to upsample the source domain or downsample the target domain to obtain better results. However, there is no need to our proposed method (SRDA-Net).

For reporting the effect of our algorithm, Fig. 4 gives the three typical example labeling results. From the visual results, we can find that the segmentation results are getting more and

more refined in our step-by-step experiments. And our SRDA-Net obtains the finer segmentation results.

### E. SRDA-Net vs. Cyclegan

Fig. 5 shows the qualitative super-resolution results with style transfer of source domain images from CycleGAN and SRDA-Net. Despite of superimposing the style of target domain, CycleGAN generates monotonous and unnatural textures, like buildings in Fig. 5. Moreover, we find that some objects in the results of CycleGAN get distorted, like cars in Fig. 5. The reason is that upsampled source domain images are blurry, which drops some information. SRDA-Net employs semantic category priors to help capture the characteristics of each category, leading to more natural and realistic textures. And by adversarial training, the super-resolution images of SRDA-Net simultaneously achieve style conversion.

## V. CONCLUSION

In this paper, we propose a novel UDA framework named SRDA-Net to explicitly address the adaptive research in the field of semantic segmentation with different resolution. To be specific, a multi-task model for super-resolution and semantic segmentation is built, named RS, which eliminating the difference of resolution between source and target domains. In addition, the pixel-level and output-space domain classifiers are designed to guide the RS model to learn domain-invariant features by the adversarial learning, which can reduce the domain gap effectively. In order to prove the effectiveness of our framework, we construct two datasets which have different resolutions in their source and target domains: Mass-*Inria* and *Vaih-Pots*. Extensive experiments demonstrate the effectiveness of our model when domain adaptation involving the resolution difference.

## REFERENCES

- [1] K. Yang, Z. Liu, Q. Lu, and G.-S. Xia, “Multi-scale weighted branch network for remote sensing image classification,” in *The IEEE Conference on Computer Vision and Pattern Recognition (CVPR) Workshops*, June 2019.
- [2] J. Richards and X. Jia, *Remote Sensing Digital Image Analysis*, 01 1999.
- [3] X. Jia, *Remote sensing digital image analysis: an introduction*. Springer Berlin Heidelberg, 2006.
- [4] J. Long, E. Shelhamer, and T. Darrell, “Fully convolutional networks for semantic segmentation,” in *Proceedings of the IEEE conference on computer vision and pattern recognition*, 2015, pp. 3431–3440.
- [5] V. Badrinarayanan, A. Kendall, and R. Cipolla, “Segnet: A deep convolutional encoder-decoder architecture for image segmentation,” *IEEE transactions on pattern analysis and machine intelligence*, vol. 39, no. 12, pp. 2481–2495, 2017.
- [6] H. Zhao, J. Shi, X. Qi, X. Wang, and J. Jia, “Pyramid scene parsing network,” in *Proceedings of the IEEE conference on computer vision and pattern recognition*, 2017, pp. 2881–2890.
- [7] L.-C. Chen, G. Papandreou, I. Kokkinos, K. Murphy, and A. L. Yuille, “Deeplab: Semantic image segmentation with deep convolutional nets, atrous convolution, and fully connected crfs,” *IEEE transactions on pattern analysis and machine intelligence*, vol. 40, no. 4, pp. 834–848, 2017.
- [8] C. Liu, L.-C. Chen, F. Schroff, H. Adam, W. Hua, A. L. Yuille, and L. Fei-Fei, “Auto-deeplab: Hierarchical neural architecture search for semantic image segmentation,” in *Proceedings of the IEEE Conference on Computer Vision and Pattern Recognition*, 2019, pp. 82–92.
- [9] B. Pan, X. Xu, Z. Shi, N. Zhang, H. Luo, and X. Lan, “Dssnet: A simple dilated semantic segmentation network for hyperspectral imagery classification,” *IEEE Geoscience and Remote Sensing Letters*, pp. 1–5, 2020.
- [10] B. Sun, J. Feng, and K. Saenko, “Return of frustratingly easy domain adaptation,” in *Thirtieth AAAI Conference on Artificial Intelligence*, 2016.
- [11] J. Hoffman, D. Wang, F. Yu, and T. Darrell, “Fcns in the wild: Pixel-level adversarial and constraint-based adaptation,” *arXiv preprint arXiv:1612.02649*, 2016.
- [12] Y. Zhang, Z. Qiu, T. Yao, D. Liu, and T. Mei, “Fully convolutional adaptation networks for semantic segmentation,” in *Proceedings of the IEEE Conference on Computer Vision and Pattern Recognition*, 2018, pp. 6810–6818.
- [13] Z. Wu, X. Wang, J. E. Gonzalez, T. Goldstein, and L. S. Davis, “Ace: Adapting to changing environments for semantic segmentation,” in *Proceedings of the IEEE International Conference on Computer Vision*, 2019, pp. 2121–2130.
- [14] Z. Wu, X. Han, Y.-L. Lin, M. Gokhan Uzunbas, T. Goldstein, S. Nam Lim, and L. S. Davis, “Dcan: Dual channel-wise alignment networks for unsupervised scene adaptation,” in *Proceedings of the European Conference on Computer Vision (ECCV)*, 2018, pp. 518–534.
- [15] X. Zhu, H. Zhou, C. Yang, J. Shi, and D. Lin, “Penalizing top performers: Conservative loss for semantic segmentation adaptation,” in *Proceedings of the European Conference on Computer Vision (ECCV)*, 2018, pp. 568–583.
- [16] Y. Li, L. Yuan, and N. Vasconcelos, “Bidirectional learning for domain adaptation of semantic segmentation,” in *Proceedings of the IEEE Conference on Computer Vision and Pattern Recognition*, 2019, pp. 6936–6945.
- [17] T.-H. Vu, H. Jain, M. Bucher, M. Cord, and P. Pérez, “Dada: Depth-aware domain adaptation in semantic segmentation,” in *Proceedings of the IEEE International Conference on Computer Vision*, 2019, pp. 7364–7373.
- [18] Y.-H. Tsai, W.-C. Hung, S. Schulter, K. Sohn, M.-H. Yang, and M. Chandraker, “Learning to adapt structured output space for semantic segmentation,” in *Proceedings of the IEEE Conference on Computer Vision and Pattern Recognition*, 2018, pp. 7472–7481.
- [19] T.-H. Vu, H. Jain, M. Bucher, M. Cord, and P. Pérez, “Advent: Adversarial entropy minimization for domain adaptation in semantic segmentation,” in *Proceedings of the IEEE Conference on Computer Vision and Pattern Recognition*, 2019, pp. 2517–2526.
- [20] Z. Zhang, K. Doi, A. Iwasaki, and G. Xu, “Unsupervised domain adaptation of high-resolution aerial images via correlation alignment and self training,” *IEEE Geoscience and Remote Sensing Letters*, pp. 1–5, 2020.
- [21] W. Liu and R. Qin, “A multikernel domain adaptation method for unsupervised transfer learning on cross-source and cross-region remote sensing data classification,” *IEEE Transactions on Geoscience and Remote Sensing*, pp. 1–11, 2020.
- [22] L. Yan, B. Fan, H. Liu, C. Huo, S. Xiang, and C. Pan, “Triplet adversarial domain adaptation for pixel-level classification of vhr remote sensing images,” *IEEE Transactions on Geoscience and Remote Sensing*, vol. 58, no. 5, pp. 3558–3573, 2020.
- [23] J. Zhang, J. Liu, B. Pan, and Z. Shi, “Domain adaptation based on correlation subspace dynamic distribution alignment for remote sensing image scene classification,” *IEEE Transactions on Geoscience and Remote Sensing*, pp. 1–11, 2020.
- [24] X. Wang, K. Yu, C. Dong, and C. Change Loy, “Recovering realistic texture in image super-resolution by deep spatial feature transform,” in *Proceedings of the IEEE conference on computer vision and pattern recognition*, 2018, pp. 606–615.
- [25] M. S. Rad, B. Bozorgtabar, U.-V. Marti, M. Basler, H. K. Ekenel, and J.-P. Thiran, “Srobb: Targeted perceptual loss for single image super-resolution,” in *Proceedings of the IEEE International Conference on Computer Vision*, 2019, pp. 2710–2719.
- [26] S. Lei, Z. Shi, X. Wu, B. Pan, X. Xu, and H. Hao, “Simultaneous super-resolution and segmentation for remote sensing images,” in *IGARSS 2019-2019 IEEE International Geoscience and Remote Sensing Symposium*. IEEE, 2019, pp. 3121–3124.
- [27] I. Goodfellow, J. Pouget-Abadie, M. Mirza, B. Xu, D. Warde-Farley, S. Ozair, A. Courville, and Y. Bengio, “Generative adversarial nets,” in *Advances in neural information processing systems*, 2014, pp. 2672–2680.
- [28] R. Mottaghi, X. Chen, X. Liu, N.-G. Cho, S.-W. Lee, S. Fidler, R. Urtasun, and A. Yuille, “The role of context for object detection and semantic segmentation in the wild,” in *Proceedings of the IEEE Conference on Computer Vision and Pattern Recognition*, 2014, pp. 891–898.
- [29] M. Cordts, M. Omran, S. Ramos, T. Rehfeld, M. Enzweiler, R. Benenson, U. Franke, S. Roth, and B. Schiele, “The cityscapes dataset for

semantic urban scene understanding,” in *Proc. of the IEEE Conference on Computer Vision and Pattern Recognition (CVPR)*, 2016.

[30] G. Lin, C. Shen, A. Van Den Hengel, and I. Reid, “Efficient piecewise training of deep structured models for semantic segmentation,” in *Proceedings of the IEEE conference on computer vision and pattern recognition*, 2016, pp. 3194–3203.

[31] S. Chandra, N. Usunier, and I. Kokkinos, “Dense and low-rank gaussian crfs using deep embeddings,” in *Proceedings of the IEEE International Conference on Computer Vision*, 2017, pp. 5103–5112.

[32] W. T. Freeman, E. C. Pasztor, and O. T. Carmichael, “Learning low-level vision,” *International journal of computer vision*, vol. 40, no. 1, pp. 25–47, 2000.

[33] C. Dong, C. C. Loy, K. He, and X. Tang, “Learning a deep convolutional network for image super-resolution,” in *European conference on computer vision*. Springer, 2014, pp. 184–199.

[34] Y. Zhang, Y. Tian, Y. Kong, B. Zhong, and Y. Fu, “Residual dense network for image super-resolution,” in *Proceedings of the IEEE conference on computer vision and pattern recognition*, 2018, pp. 2472–2481.

[35] Z. Li, J. Yang, Z. Liu, X. Yang, G. Jeon, and W. Wu, “Feedback network for image super-resolution,” in *Proceedings of the IEEE Conference on Computer Vision and Pattern Recognition*, 2019, pp. 3867–3876.

[36] J. Johnson, A. Alahi, and L. Fei-Fei, “Perceptual losses for real-time style transfer and super-resolution,” in *European conference on computer vision*. Springer, 2016, pp. 694–711.

[37] C. Ledig, L. Theis, F. Huszár, J. Caballero, A. Cunningham, A. Acosta, A. Aitken, A. Tejani, J. Totz, Z. Wang *et al.*, “Photo-realistic single image super-resolution using a generative adversarial network,” in *Proceedings of the IEEE conference on computer vision and pattern recognition*, 2017, pp. 4681–4690.

[38] Z. Zou, T. Shi, W. Li, Z. Zhang, and Z. Shi, “Do game data generalize well for remote sensing image segmentation?” *Remote Sensing*, vol. 12, no. 2, p. 275, 2020.

[39] Y. Zhang, P. David, and B. Gong, “Curriculum domain adaptation for semantic segmentation of urban scenes,” in *Proceedings of the IEEE International Conference on Computer Vision*, 2017, pp. 2020–2030.

[40] Q. Lian, F. Lv, L. Duan, and B. Gong, “Constructing self-motivated pyramid curriculums for cross-domain semantic segmentation: A non-adversarial approach,” in *Proceedings of the IEEE International Conference on Computer Vision*, 2019, pp. 6758–6767.

[41] Y. Zhang, P. David, H. Foroosh, and B. Gong, “A curriculum domain adaptation approach to the semantic segmentation of urban scenes,” *IEEE transactions on pattern analysis and machine intelligence*, 2019.

[42] K.-H. Lee, G. Ros, J. Li, and A. Gaidon, “Spigan: Privileged adversarial learning from simulation,” *arXiv preprint arXiv:1810.03756*, 2018.

[43] L. Wang, Y. Wang, Z. Liang, Z. Lin, J. Yang, W. An, and Y. Guo, “Learning parallax attention for stereo image super-resolution,” in *Proceedings of the IEEE Conference on Computer Vision and Pattern Recognition*, 2019, pp. 12250–12259.

[44] W. Shi, J. Caballero, F. Huszár, J. Totz, A. P. Aitken, R. Bishop, D. Rueckert, and Z. Wang, “Real-time single image and video super-resolution using an efficient sub-pixel convolutional neural network.”

[45] T.-Y. Lin, P. Dollár, R. Girshick, K. He, B. Hariharan, and S. Belongie, “Feature pyramid networks for object detection,” in *Proceedings of the IEEE conference on computer vision and pattern recognition*, 2017, pp. 2117–2125.

[46] D. Kotovenko, A. Sanakoyeu, P. Ma, S. Lang, and B. Ommer, “A content transformation block for image style transfer,” in *The IEEE Conference on Computer Vision and Pattern Recognition (CVPR)*, June 2019.

[47] C. Li and M. Wand, “Precomputed real-time texture synthesis with markovian generative adversarial networks,” in *European conference on computer vision*. Springer, 2016, pp. 702–716.

[48] V. Mnih, “Machine learning for aerial image labeling,” Ph.D. dissertation, University of Toronto, 2013.

[49] E. Maggiori, Y. Tarabalka, G. Charpiat, and P. Alliez, “Can semantic labeling methods generalize to any city? the inria aerial image labeling benchmark,” in *IEEE International Geoscience and Remote Sensing Symposium (IGARSS)*. IEEE, 2017.

[50] K. He, X. Zhang, S. Ren, and J. Sun, “Deep residual learning for image recognition,” in *Proceedings of the IEEE conference on computer vision and pattern recognition*, 2016, pp. 770–778.

[51] J.-Y. Zhu, T. Park, P. Isola, and A. A. Efros, “Unpaired image-to-image translation using cycle-consistent adversarial networks,” in *Proceedings of the IEEE international conference on computer vision*, 2017, pp. 2223–2232.